

# Optimized up-down asymmetry to drive fast intrinsic rotation in tokamaks

Justin Ball,<sup>1,2,3,\*</sup> Felix I. Parra,<sup>1,2</sup> Matt Landreman,<sup>4</sup> and Michael Barnes<sup>1,2</sup>

<sup>1</sup>Rudolf Peierls Centre for Theoretical Physics, University of Oxford, Oxford OX1 3NP, United Kingdom

<sup>2</sup>Culham Centre for Fusion Energy, Culham Science Centre, Abingdon OX14 3DB, United Kingdom

<sup>3</sup>Swiss Plasma Center, École Polytechnique Fédérale de Lausanne, 1015 Lausanne, Switzerland

<sup>4</sup>Institute for Research in Electronics and Applied Physics,  
University of Maryland, College Park, Maryland 20742, USA

(Dated: March 10, 2017)

Breaking the up-down symmetry of the tokamak poloidal cross-section can significantly increase the spontaneous rotation due to turbulent momentum transport. In this work, we optimize the shape of flux surfaces with both tilted elongation and tilted triangularity in order to maximize this drive of intrinsic rotation. Nonlinear gyrokinetic simulations demonstrate that adding optimally-tilted triangularity can double the momentum transport of a tilted elliptical shape. This work indicates that tilting the elongation and triangularity in an ITER-like device can reduce the energy transport and drive intrinsic rotation with an Alfvén Mach number on the order of 1%. This rotation is four times larger than the rotation expected in ITER and is sufficient to stabilize MHD instabilities. It is shown that this optimal shape can be created using the shaping coils of several experiments.

PACS numbers: 52.25.Fi, 52.30.Cv, 52.30.Gz, 52.35.Ra, 52.55.Fa, 52.65.Tt

*Introduction.* — Bulk toroidal rotation is generally beneficial for plasma performance in tokamaks, a toroidally-symmetric magnetic fusion device. Typically, rotation with an Alfvén Mach number  $M_A \approx 1\%$  [1] (or a Mach number  $M_S \approx 5\%$  using the definition of Ref. [2]) can stabilize dangerous magnetohydrodynamic (MHD) modes [3, 4]. Higher levels of rotation can combat turbulence [5, 6]. Unfortunately, the mechanisms that drive toroidal rotation in existing experiments do not appear to scale well to future high-performance devices (i.e. larger devices with stronger magnetic fields). One such device, the ITER experiment [7], is presently under construction.

Typically, rotation is driven by pushing the plasma using external injection of momentum. This is commonly done with beams of neutral particles, which enable existing experiments to achieve toroidal rotation with  $M_A \approx 3\%$  (or  $M_S \approx 15\%$ ) [3]. However, due to ITER’s larger size, external injection is only expected to drive rotation with  $M_A \approx 0.3\%$  (or  $M_S \approx 1.5\%$ ) [1], significantly less than what is needed for MHD stabilization.

An attractive alternative is “intrinsic” rotation, or rotation spontaneously generated by the turbulent transport of momentum. Turbulence enables the plasma to push against the surrounding vacuum vessel and external magnets as well as move momentum between the nested magnetic flux surfaces (see Fig. 1). Unfortunately, the intrinsic rotation in existing experiments is observed to be fairly modest, typically with  $M_A \lesssim 1\%$  (or  $M_S \lesssim 5\%$ ) [8]. This has been explained by noting a particular symmetry [9] of the gyrokinetic model, a theoretical model that is thought to accurately describe turbulence in tokamaks. This symmetry constrains the intrinsic rotation to be small in  $\rho_* \equiv \rho_i/a \ll 1$ , the ratio of the ion gyroradius  $\rho_i$  to the tokamak minor radius  $a$ . However, it is broken if the magnetic equilibrium is up-down asymmetric (i.e.

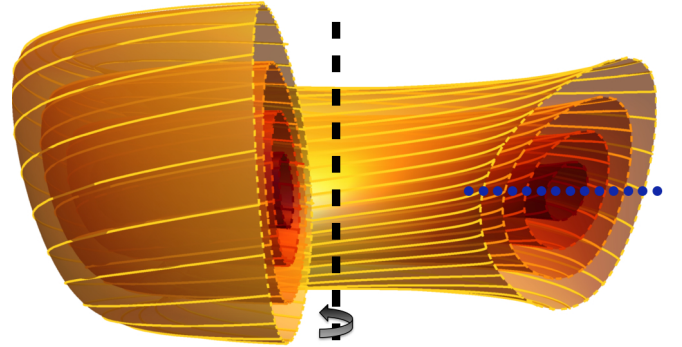


FIG. 1. A cutaway view of the flux surfaces in the “optimal” magnetic geometry (i.e. the equilibrium that we expect to maximize intrinsic toroidal rotation generated by up-down asymmetry), shown with the midplane (blue, dotted) and axis of toroidal symmetry (black, dashed).

is not mirror symmetric about the midplane as shown in Fig. 1). Subsequent numerical [10, 11] and experimental [12] work using flux surfaces with tilted elliptical shapes suggests that up-down asymmetry is a feasible method to generate the present experimentally-measured rotation levels in future larger devices (which have smaller values of  $\rho_*$ ).

Recently, a series of analytic arguments have been formulated concerning the ability of different up-down asymmetric flux surface shapes to drive intrinsic rotation. MHD analysis has shown that externally-applied shaping with a large poloidal mode number  $m \gg 1$  does not penetrate effectively throughout the plasma, but only shapes an exponentially thin layer at the edge [13]. Furthermore, another symmetry of the gyrokinetic model, a poloidal tilting symmetry, has been demonstrated in the limit of high-order flux surface shaping [14]. The

tilting symmetry implies that mirror symmetric flux surfaces (i.e. flux surfaces that have mirror symmetry about at least one line in the poloidal plane) drive momentum transport that is exponentially small in  $m \gg 1$ . However, we can break tilting symmetry using non-mirror symmetric flux surface shapes [15, 16] (i.e. shapes that do not have mirror symmetry about any line in the poloidal plane). This allows rotation to be driven by the direct interaction between different shaping modes (irrespective of toroidicity).

Taken together all these arguments motivate up-down asymmetric flux surface shapes with the lowest possible poloidal mode numbers. Additionally, it is important to explore the effect of non-mirror symmetry as it may enhance the rotation drive. In this work we will consider flux surfaces with both elongation and triangularity and allow the two shaping effects to be tilted independently in order to break mirror symmetry. These two modes,  $m = 2$  and  $m = 3$ , are the lowest order modes that can be created by external shaping coils. The  $m = 1$  mode (i.e. the Shafranov shift) is not directly controlled by external magnets and has already been considered in Ref. [17]. By varying these two tilt angles, we will optimize the geometry to drive the fastest intrinsic rotation and look for geometries that directly improve the energy confinement time, irrespective of rotation.

*Magnetic equilibrium.* — Before we can simulate turbulence, we must first specify the magnetic equilibrium. Due to axisymmetry, the general form of the magnetic field in a tokamak is given by

$$\vec{B} = I(\psi) \vec{\nabla} \zeta + \vec{\nabla} \zeta \times \vec{\nabla} \psi, \quad (1)$$

where  $\zeta$  is the toroidal angle and  $I(\psi)$  (which is closely related to the poloidal plasma current) controls the toroidal field strength. The magnetic flux surfaces (see Fig. 1) are contours of the stream function  $\psi$  (which is the poloidal magnetic flux divided by  $2\pi$ ). We will motivate experimentally-practical flux surface shapes using solutions to the Grad-Shafranov equation

$$R^2 \vec{\nabla} \cdot \left( \frac{\vec{\nabla} \psi}{R^2} \right) = -\mu_0 j_\zeta R, \quad (2)$$

which governs the tokamak equilibrium [18]. Here  $R$  is the major radial coordinate,  $\mu_0$  is the permeability of free space, and  $j_\zeta$  is the toroidal plasma current density. To find a simple and realistic solution, we assume  $j_\zeta$  is uniform and expand in the limit of large aspect ratio (given the typical orderings for a low  $\beta$ , ohmically heated tokamak [19]). In this context, Eq. (2) is solved by

$$\psi_N(r, \theta) = r_N^2 + \sum_{m=2}^{\infty} C_{Nm} r_N^m \cos(m(\theta + \theta_m)), \quad (3)$$

where we have normalized all lengths to the tokamak minor radius  $a$ , all magnetic fields to  $\mu_0 j_\zeta R_0/4$ , and indicated these normalized quantities by the subscript  $N$ .

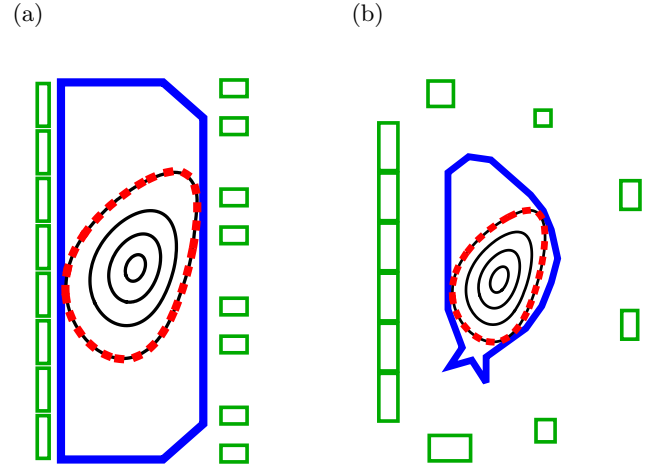


FIG. 2. Global free-boundary MHD equilibria (black, solid) created by the (a) TCV or (b) ITER poloidal shaping coils (green, rectangles) compared to the target “optimal” boundary shape (red, dashed, thick) along with the first wall (blue, solid, thick).

Here  $r$  is the distance from the magnetic axis (i.e. the line enclosed by all flux surfaces),  $\theta$  is the usual cylindrical poloidal angle,  $C_m$  controls the strength of each shaping mode,  $\theta_m$  is the mode tilt angle, and  $R_0$  is the major radial location of the magnetic axis. By applying a boundary condition with only the  $m = 2$  and  $m = 3$  modes, Eq. (3) becomes a cubic in  $r$  that we can invert to find  $r_N(\psi_N, \theta)$ , the shape of each flux surface in the equilibrium.

We expect this geometry specification to produce experimentally-practical flux surface shapes to lowest order in the large aspect ratio expansion. To show why, we first note that the vacuum and constant current density solutions to Eq. (2) are identical, except for the inhomogeneous  $r_N^2$  term. From the  $r_N \rightarrow 0$  limit of Eq. (3), we can see that low  $m$  shaping modes are exponentially more effective (in the  $m \gg 1$  limit) at maintaining their effect over large distances [13]. Hence, if the shaping coils are very far from the plasma (as would be preferable in a reactor), the only feasible shapes are those composed of low-order modes in Eq. (3).

To confirm the experimental feasibility of these shapes, we created the “optimal” flux surface boundary shape using experimental coil sets in two ways. First, we used the FBT code [20] (a free boundary MHD equilibrium code used to design magnetic geometries for the TCV experiment [21]) to produce the configuration shown in Fig. 2(a). This equilibrium respects all TCV coil limits for values of the plasma current up to 400 kA. Second, using the least-squares minimization algorithm used for Fig. 9 of Ref. [22], we showed that the ITER coil set [7] is capable of matching the “optimal” shape (see Fig.

2(b)).

*Intrinsic rotation driven by turbulence.* — To model turbulent transport we will use gyrokinetics [23–32] because experimental measurements [33] indicate that it accurately treats turbulence in the core of tokamaks. Gyrokinetics is a fully-kinetic description based on an expansion of the Fokker-Planck and Maxwell’s equations in  $\rho_* \ll 1$ . It specifically investigates behavior much slower than the ion gyrofrequency, but still allows the size of the turbulent eddies perpendicular to the magnetic field to be comparable to the gyroradius. In this regime, we can average over the fast particle gyromotion using the gyroaverage  $\langle \dots \rangle_\varphi$ . This removes one dimension of velocity space as well as the gyrofrequency timescale, which makes the model computationally tractable.

To further simplify, we will assume the turbulent fluctuations are electrostatic (i.e. the magnetic pressure dominates the thermal pressure) and neglect particle collisions (i.e. the temperature is sufficiently high). Additionally, we are interested in mechanisms that cause a stationary plasma to begin rotating, so we will take the rotation and rotation shear to be zero (i.e.  $\Omega_\zeta = d\Omega_\zeta/d\psi = 0$ ). Lastly, we will separate the perturbation in the distribution function due to turbulence  $\delta f_s$  from the background distribution function  $F_{Ms}$ , which we assume to be Maxwellian. Here the subscript  $s$  indicates either the ion or electron species.

Given these assumptions, the gyrokinetic equation is given by

$$\frac{\partial \langle \delta f_s \rangle_\varphi}{\partial t} + \left( v_{||} \hat{b} + \vec{v}_B + \langle \vec{v}_E \rangle_\varphi \right) \cdot \vec{\nabla} \left( \langle \delta f_s \rangle_\varphi + \frac{Z_s e \langle \phi \rangle_\varphi}{T_s} F_{Ms} \right) = - \langle \vec{v}_E \rangle_\varphi \cdot \vec{\nabla} F_{Ms}, \quad (4)$$

which is solved together with the gyroaveraged, perturbed quasineutrality equation (i.e. Gauss’s law) for  $\langle \delta f_s \rangle_\varphi$  and  $\langle \phi \rangle_\varphi$ , the gyroaveraged electrostatic potential. Here  $t$  is the time,  $v_{||}$  is the component of the velocity parallel to the magnetic field unit vector  $\hat{b}$ ,  $\vec{v}_B$  is the magnetic drift velocity,  $\vec{v}_E$  is the  $\vec{E} \times \vec{B}$  drift velocity,  $Z_s$  is the particle charge number,  $e$  is the proton charge, and  $T_s$  is the background temperature.

By running the code GS2 [34] on supercomputers, we can solve the gyrokinetic equation in flux tube, a long narrow simulation domain that follows a single magnetic field line on a single flux surface. This allows us to calculate the radial fluxes of energy and toroidal angular momentum according to

$$Q_s \equiv \left\langle \int_\psi dS \int d^3v \left( \frac{m_s v^2}{2} \right) \vec{v}_E \cdot \frac{\vec{\nabla} \psi}{|\vec{\nabla} \psi|} \delta f_s \right\rangle_t \quad (5)$$

$$\Pi_\zeta \equiv \left\langle \int_\psi dS \int d^3v \left( m_i R^2 \vec{v} \cdot \vec{\nabla} \zeta \right) \vec{v}_E \cdot \frac{\vec{\nabla} \psi}{|\vec{\nabla} \psi|} \delta f_i \right\rangle_t \quad (6)$$

respectively, where  $m_s$  is the particle mass,  $v$  is the speed,  $\int_\psi dS$  indicates an integral over the flux surface, and  $\langle \dots \rangle_t$  indicates a time average over the turbulent timescale.

In general, to calculate the rotation profile in statistical steady-state you must invert  $\Pi_\zeta(\Omega_\zeta, d\Omega_\zeta/d\psi) = 0$  on every flux surface [35]. However, we can calculate a simple estimate of the level of rotation using local values of  $\Pi_\zeta$  and  $Q_i$  [17]. First, we assume that the energy flux is dominated by the diffusion of a temperature gradient [36] (i.e.  $Q_i = -D_Q n_i dT_i/d\psi$ ). Then, expanding  $\Pi_\zeta(\Omega_\zeta, d\Omega_\zeta/d\psi) = 0$  around  $\Omega_\zeta = d\Omega_\zeta/d\psi = 0$  and neglecting the term proportional to  $\Omega_\zeta$  (which can only enhance the rotation [37]), gives  $\Pi_\zeta(0, 0) = D_{\Pi} n_i m_i R_0^2 d\Omega_\zeta/d\psi$ . Here  $n_i$  is the ion number density, while  $D_Q$  and  $D_{\Pi}$  are the energy and momentum diffusion coefficients respectively. We can couple the energy and momentum transport by assuming a constant turbulent Prandtl number  $Pr \equiv D_{\Pi}/D_Q \approx 0.7$  [11, 38], producing the estimate

$$\frac{R_0}{v_{th,i}} \frac{d\Omega_\zeta}{d\psi} \approx \frac{-1}{2Pr} \left( \frac{v_{th,i} \Pi_\zeta}{R_0 Q_i} \right) \frac{d}{d\psi} \ln(T_i), \quad (7)$$

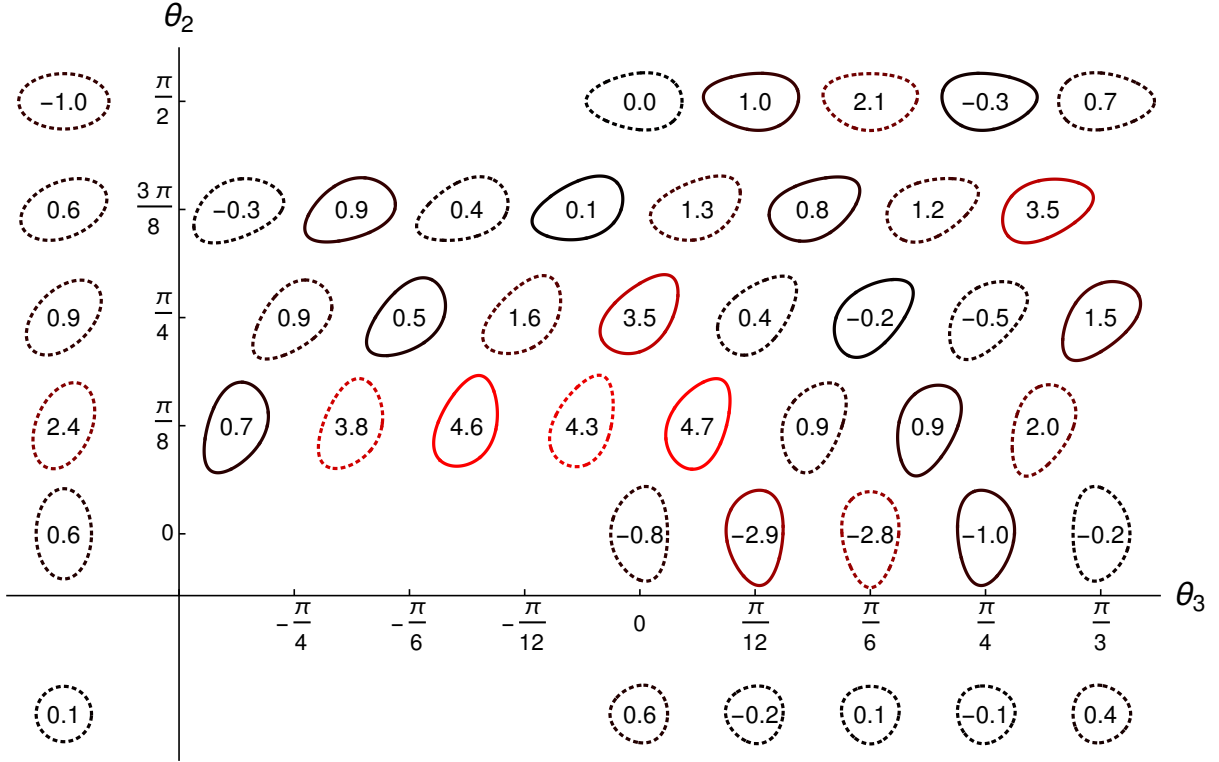
where  $v_{th,i}$  is the ion thermal velocity. We see that, by finding the shape that maximizes  $\Pi_\zeta/Q_i$  at  $\Omega_\zeta = d\Omega_\zeta/d\psi = 0$ , we can maximize the intrinsic rotation.

*Numerical results.* — To investigate the momentum transport in flux surfaces with both elongation and triangularity, we will perform a two dimensional scan in  $\theta_2$  and  $\theta_3$ . We choose to fix  $C_{N2} = 0.45$  and  $C_{N3} = 0.10$  because these values approximate the ITER boundary shape when  $\theta_2 = 0$  and  $\theta_3 = \pi/3$ . Instead of  $\psi_N$ , we use the real-space flux surface label  $\rho$ , which is defined by  $\psi_N(\rho) = \rho^2 + C_{N2}\rho^2 + C_{N3}\rho^3$  and corresponds to the value of  $r_N$  at the outboard midplane if the two shaping effects were untitled. By setting  $\rho = 0.75$  we select a flux surface that is in the core, but is close enough to the boundary to have substantial triangularity. The major radius  $R_0 = 3$ , safety factor  $q = 1.4$ , magnetic shear  $\hat{s} \equiv (\rho/q) dq/d\rho = 0.8$ , and background density gradient  $d\ln(n_s)/d\rho = -0.733$  are taken from the widely-used Cyclone base case [39]. Because the flux surfaces are so strongly shaped, we will use a large background temperature gradient of  $d\ln(T_s)/d\rho = -3.0$  to ensure that the turbulence is driven unstable.

Because of the strong shaping, these simulations are computationally expensive. Properly resolving the sharp poloidal structure required a fine poloidal grid with 128 grid points, a factor of four larger than conventional.

Fig. 3(a) shows how the intrinsic rotation generated by the two-mode geometries compares with that generated by flux surfaces with only elongation or triangularity. We see that configurations shaped by only elongation produce significant momentum transport, unlike configurations with only triangularity. However, the “optimal” two-mode geometry (i.e. the  $\theta_2 = \pi/8$ ,  $\theta_3 = \pi/24$  case)

(a)



(b)

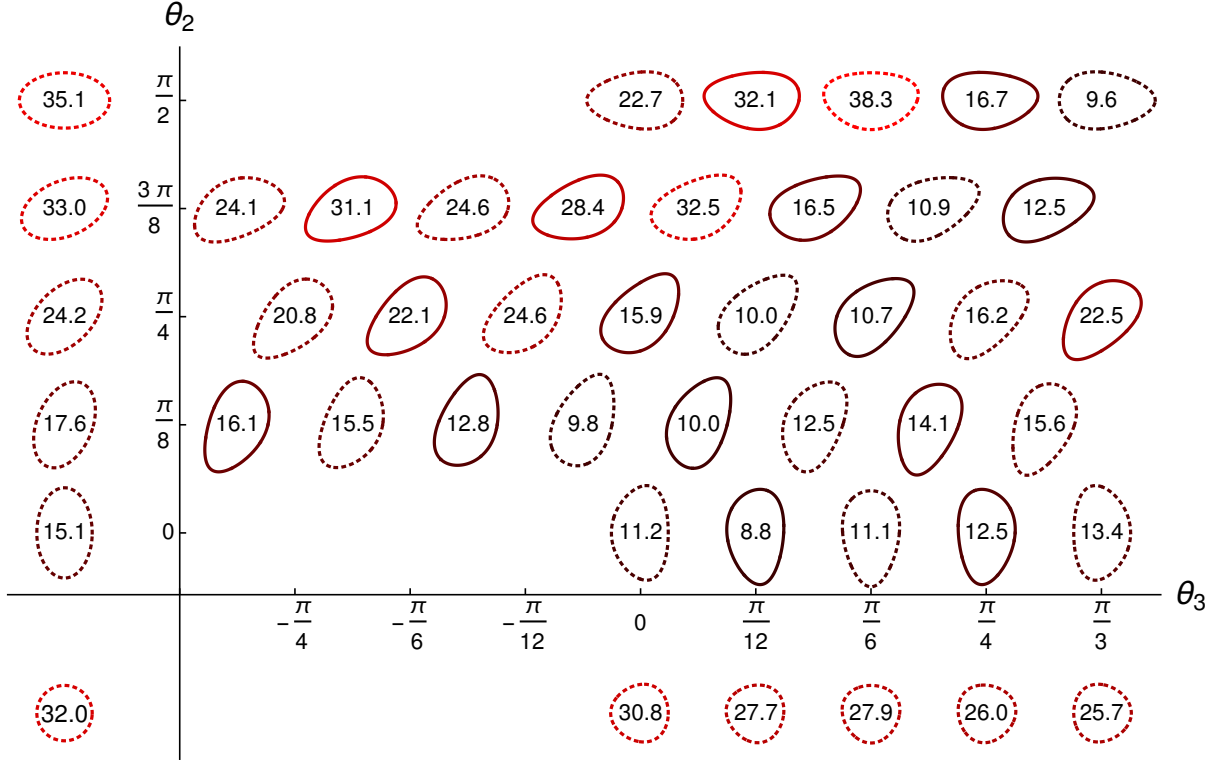


FIG. 3. Values of (a) the normalized momentum transport  $100 \times (v_{th,i}/R_0) \Pi_{\zeta}/Q_i$  and (b) the total energy flux  $(Q_i + Q_e)/Q_{gB}$  are indicated by the numbers/colors for various non-mirror symmetric (solid lines) and mirror symmetric (dotted lines) flux surfaces created with elongation and triangularity. For comparison, purely elongated flux surfaces are shown in quadrant II, a circular flux surface is shown in quadrant III, and purely triangular flux surfaces are shown in quadrant IV. Repeating several of these simulations indicates that the statistical error from averaging over the turbulent timescale is  $\pm 0.5$  for the energy flux and  $\pm 1$  for the normalized momentum transport (which is consistent with the small, but non-zero results of the up-down symmetric geometries).

has almost double the momentum transport of any single-mode geometry. Performing an additional simulation of the “optimal” geometry with  $(R_0/v_{th,i})d\Omega_\zeta/d\rho = 0.1$  confirmed that  $\Pi_\zeta \approx 0$  as predicted by Eq. (7). If we assume that  $(v_{th,i}/R_0)\Pi_\zeta/Q_i$  is uniform across the flux surfaces that have a substantial temperature gradient, then we can integrate Eq. (7). Without any edge rotation, this estimate predicts that the on-axis intrinsic rotation in the “optimal” geometry will have an  $M_S \approx 7\%$ . This value corresponds to  $M_A \approx 1.2\%$ , given an ITER-like value of  $\beta = 0.06$  (i.e. the ratio of the thermal and magnetic pressures). This level of rotation is roughly what is needed to stabilize MHD modes.

One possible explanation for the large difference between the elliptical and two-mode geometries is the breaking of flux surface mirror symmetry. We know that breaking mirror symmetry allows the interaction of different shaping effects to directly drive momentum (which would be the dominant mechanism in a cylindrical device). However, for the aspect ratio of these simulations, this effect appears to be fairly modest. Of the four configurations with the most momentum transport, two of them are mirror symmetric. Instead, it appears that the intrinsic rotation drive is dominated by the direct interaction of elongation and triangularity with toroidicity.

Fig. 3(b) shows that the best performing two-mode geometries directly stabilize turbulence and increase the confinement time, irrespective of rotation. In fact, the “optimal” geometry has 25% less energy transport than the ITER-like shape (i.e.  $\theta_2 = 0$  and  $\theta_3 = \pi/3$ ). Furthermore, the turbulence can be completely stabilized at the standard Cyclone base case temperature gradient of  $a/L_{Ts} = 2.3$ . Hence, not only can the energy transport be reduced, but the critical gradient can be increased substantially. *acknowledgments*

*Conclusions.* — This work indicates that up-down asymmetry can drive sufficient intrinsic rotation to stabilize MHD modes in large devices. Our analysis has identified the optimal tilt angles (i.e.  $\theta_2 = \pi/8$  and  $\theta_3 = \pi/24$ ) to maximize the rotation for typical values of elongation and triangularity. Furthermore, we have shown that this shape can be created experimentally and has 25% less turbulent energy transport than the nominal ITER-like shape.

*Acknowledgments.* — The authors would like to thank S. Brunner, I. Pusztai, M. Wensing, H. Reimerdes and P. Helander for useful discussions pertaining to this work. This work was funded in part by the RCUK Energy Programme (grant number EP/I501045). It has been carried out within the framework of the EUROfusion Consortium and has received funding from the Euratom research and training program 2014–2018 under Grant Agreement No. 633053. Computing time for this work was provided by the Helios supercomputer at IFERC-CSC under the projects SPIN, TRIN, and GKMSC. Additionally, we acknowledge the CINECA award under the

ISCRA initiative, for the availability of high performance computing resources and support.

---

\* Justin.Ball@epfl.ch

- [1] Y. Liu, A. Bondeson, Y. Gribov, and A. Polevoi. Stabilization of resistive wall modes in ITER by active feedback and toroidal rotation. *Nucl. Fusion*, 44(2):232, 2004.
- [2] J. C. Hillesheim, F. I. Parra, M. Barnes, N. A. Crocker, H. Meyer, W. A. Peebles, R. Scannell, A. Thornton, and the MAST Team. Dependence of intrinsic rotation reversals on collisionality in MAST. *Nucl. Fusion*, 55(3):032003, 2015.
- [3] A.M. Garofalo, E.J. Strait, L.C. Johnson, R.J. La Haye, E.A. Lazarus, G.A. Navratil, M. Okabayashi, J.T. Scoville, T.S. Taylor, and A.D. Turnbull. Sustained stabilization of the resistive-wall mode by plasma rotation in the DIII-D tokamak. *Phys. Rev. Lett.*, 89(23):235001, 2002.
- [4] H. Reimerdes, T.C. Hender, S.A. Sabbagh, J.M. Bialek, M.S. Chu, A.M. Garofalo, M.P. Gryaznevich, D.F. Howell, G.L. Jackson, R.J. La Haye, and others. Cross-machine comparison of resonant field amplification and resistive wall mode stabilization by plasma rotation. *Phys. Plasmas*, 13(5):56107, 2006.
- [5] C.P. Ritz, H. Lin, T.L. Rhodes, and A.J. Wootton. Evidence for confinement improvement by velocity-shear suppression of edge turbulence. *Phys. Rev. Lett.*, 65(20):2543, 1990.
- [6] K.H. Burrell. Effects of  $E \times B$  velocity shear and magnetic shear on turbulence and transport in magnetic confinement devices. *Phys. Plasmas*, 4(5):1499, 1997.
- [7] R. Aymar and others. Summary of the ITER final design report. *ITER document G A0 FDR*, 4:01, 2001.
- [8] J.E. Rice, A. Ince-Cushman, L.-G. Eriksson, Y. Sakamoto, A. Scarabosio, A. Bortolon, K.H. Burrell, B.P. Duval, C. Fenzi-Bonizec, M.J. Greenwald, and others. Inter-machine comparison of intrinsic toroidal rotation in tokamaks. *Nucl. Fusion*, 47(11):1618, 2007.
- [9] F.I. Parra, M. Barnes, and A.G. Peeters. Up-down symmetry of the turbulent transport of toroidal angular momentum in tokamaks. *Phys. Plasmas*, 18(6):062501, 2011.
- [10] Y. Camenen, A.G. Peeters, C. Angioni, F.J. Casson, W.A. Hornsby, A.P. Snodin, and D. Strintzi. Transport of Parallel Momentum Induced by Current-Symmetry Breaking in Toroidal Plasmas. *Phys. Rev. Lett.*, 102(12):125001, 2009.
- [11] J. Ball, F.I. Parra, M. Barnes, W. Dorland, G.W. Hammett, P. Rodrigues, and N.F. Loureiro. Intrinsic momentum transport in up-down asymmetric tokamaks. *Plasma Phys. Control. Fusion*, 56(9):095014, 2014.
- [12] Y. Camenen, A. Bortolon, B.P. Duval, L. Federspiel, A.G. Peeters, F.J. Casson, W.A. Hornsby, A.N. Karpushov, F. Piras, O. Sauter, and others. Experimental evidence of momentum transport induced by an up-down asymmetric magnetic equilibrium in toroidal plasmas. *Phys. Rev. Lett.*, 105(13):135003, 2010.
- [13] J. Ball. *Up-down Asymmetric Tokamaks*. PhD thesis, University of Oxford, Trinity term 2016.
- [14] J. Ball, F.I. Parra, and M. Barnes. Poloidal tilting symmetry of high order tokamak flux surface shaping in gy-

- rokinetics. *Plasma Phys. Control. Fusion*, 58(4):045023, 2016.
- [15] J. Ball and F.I. Parra. Scaling of up-down asymmetric turbulent momentum flux with poloidal shaping mode number in tokamaks. *Plasma Phys. Control. Fusion*, 58(5):055016, 2016.
- [16] J. Ball and F.I. Parra. Turbulent momentum transport due to the beating between different tokamak flux surface shaping effects. *Plasma Phys. Control. Fusion*, 59(2):024007, 2017.
- [17] J. Ball, F.I. Parra, J. Lee, and A.J. Cerfon. Effect of the Shafranov shift and the gradient of  $\beta$  on intrinsic momentum transport in up-down asymmetric tokamaks. *Plasma Phys. Control. Fusion*, 58(12):125015, 2016.
- [18] V.D. Shafranov. Plasma equilibrium in a magnetic field. *Rev. Plasma Phys.*, 2:103, 1966.
- [19] J.P. Freidberg. Ideal Magnetohydrodynamics. page 126. Plenum Press, New York, NY, 1987.
- [20] F. Hofmann. FBT-a free-boundary tokamak equilibrium code for highly elongated and shaped plasmas. *Comput. Phys. Commun.*, 48(2):207, 1988.
- [21] F. Hofmann, J.B. Lister, W. Anton, S. Barry, R. Behn, S. Bernel, G. Besson, F. Buhlmann, R. Chavan, M. Corboz, and others. Creation and control of variably shaped plasmas in TCV. *Plasma Phys. Control. Fusion*, 36(12B):B277, 1994.
- [22] M. Landreman and A.H. Boozer. Efficient magnetic fields for supporting toroidal plasmas. *Phys. Plasmas*, 23(3):032506, 2016.
- [23] X.S. Lee, J.R. Myra, and P.J. Catto. General frequency gyrokinetics. *Phys. Fluids*, 26(1):223, 1983.
- [24] W.W. Lee. Gyrokinetic approach in particle simulation. *Phys. Fluids*, 26(2):556, 1983.
- [25] D.H.E. Dubin, J.A. Krommes, C. Oberman, and W.W. Lee. Nonlinear gyrokinetic equations. *Phys. Fluids*, 26(12):3524, 1983.
- [26] T.S. Hahm. Nonlinear gyrokinetic equations for tokamak microturbulence. *Phys. Fluids*, 31(9):2670, 1988.
- [27] H. Sugama, M. Okamoto, W. Horton, and M. Wakatani. Transport processes and entropy production in toroidal plasmas with gyrokinetic electromagnetic turbulence. *Phys. Plasmas*, 3(6):2379, 1996.
- [28] H. Sugama and W. Horton. Nonlinear electromagnetic gyrokinetic equation for plasmas with large mean flows. *Phys. Plasmas*, 5(7):2560, 1998.
- [29] A.J. Brizard and T.S. Hahm. Foundations of nonlinear gyrokinetic theory. *Rev. Mod. Phys.*, 79(2):421, 2007.
- [30] F.I. Parra and P.J. Catto. Limitations of gyrokinetics on transport time scales. *Plasma Phys. Control. Fusion*, 50(6):065014, 2008.
- [31] F.I. Parra and I. Calvo. Phase-space Lagrangian derivation of electrostatic gyrokinetics in general geometry. *Plasma Phys. Control. Fusion*, 53(4):045001, 2011.
- [32] I.G. Abel, G.G. Plunk, E. Wang, M.A. Barnes, S.C. Cowley, W. Dorland, and A.A. Schekochihin. Multiscale gyrokinetics for rotating tokamak plasmas: Fluctuations, transport, and energy flows. *Rep. Prog. Phys.*, 76:116201, 2013.
- [33] G.R. McKee, C.C. Petty, R.E. Waltz, C. Fenzi, R.J. Fonck, J.E. Kinsey, T.C. Luce, K.H. Burrell, D.R. Baker, E.J. Doyle, and others. Non-dimensional scaling of turbulence characteristics and turbulent diffusivity. *Nucl. Fusion*, 41(9):1235, 2001.
- [34] W. Dorland, F. Jenko, M. Kotschenreuther, and B.N. Rogers. Electron temperature gradient turbulence. *Phys. Rev. Lett.*, 85(26):5579, 2000.
- [35] F.I. Parra and M. Barnes. Intrinsic rotation in tokamaks: Theory. *Plasma Phys. Control. Fusion*, 57(4):045002, 2015.
- [36] J.P. Freidberg. Plasma Physics and Fusion Energy. page 452. Cambridge University Press, 2007.
- [37] A.G. Peeters, C. Angioni, and D. Strintzi. Toroidal momentum pinch velocity due to the coriolis drift effect on small scale instabilities in a toroidal plasma. *Phys. Rev. Lett.*, 98(26):265003, 2007.
- [38] M. Barnes, F.I. Parra, E.G. Highcock, A.A. Schekochihin, S.C. Cowley, and C.M. Roach. Turbulent transport in tokamak plasmas with rotational shear. *Phys. Rev. Lett.*, 106(17):175004, 2011.
- [39] A.M. Dimits, G. Bateman, M.A. Beer, B.I. Cohen, W. Dorland, G.W. Hammett, C. Kim, J.E. Kinsey, M. Kotschenreuther, A.H. Kritiz, and others. Comparisons and physics basis of tokamak transport models and turbulence simulations. *Phys. Plasmas*, 7:969, 2000.